HHS Public Access

Author manuscript

ACS Appl Mater Interfaces. Author manuscript; available in PMC 2020 December 06.

Published in final edited form as:

ACS Appl Mater Interfaces. 2019 September 18; 11(37): 34463–34470. doi:10.1021/acsami.9b12342.

Surface Modification of Glass/PDMS Microfluidic Valve Assemblies Enhances Valve Electrical Resistance

Xuemin Wang[1], **Mark T. Agasid**[1], **Christopher A. Baker**[*,1,4], **Craig A. Aspinwall**[*,1,2,3]

[1]Department of Chemistry and Biochemistry, University of Arizona, Tucson, Arizona, 85721, United States

[2]BIO5 Institute, University of Arizona, Tucson, Arizona, 85721, United States

[3]Department of Biomedical Engineering, University of Arizona, Tucson, Arizona, 85721, United States

[4]Department of Chemistry, University of Tennessee, Knoxville, Tennessee, 37996, United States

Abstract

Microfluidic instrumentation offers unique advantages in biotechnology applications including reduced sample and reagent consumption, rapid mixing and reaction times, and a high degree of process automation. As dimensions decrease, the ratio of surface area to volume within a fluidic architecture increases, which gives rise to some of the unique advantages inherent to microfluidics. Thus, manipulation of surface characteristics presents a promising approach to tailor the performance of microfluidic systems. Microfluidic valves are essential components in a number of small volume applications and for automated microfluidic platforms, but rigorous evaluation of the sealing quality of these valves is often overlooked. In this work, the glass valve seat of hybrid glass/PDMS microfluidic valves was surface modified with hydrophobic silanes, octyldimethylchlorosilane (ODCS) or (tridecafluoro-1,1,2,2-tetrahydrooctyl)dimethylchlorosilane (PFDCS), to investigate the effect of surface energy on electrical resistance of valves. Valves with ODCS- or PFDCS- modified valve seats both exhibited >70-fold increases in electrical resistance (>500 GΩ) when compared to the same valve design with unmodified glass valve seats (7 ± 3 GΩ), indicative of higher sealing capacity. The opening times for valves with ODCS- or PFDCS-modified valve seats was ca. 5x shorter compared to unmodified valve seats, whereas the closing time was up to 8x longer for modified valve seats, though the total closing time was ≤1.5 s, compatible with numerous microfluidic valving applications. Surface modified valves assemblies offered sufficient electrical resistance to isolate sub-pA current signals resulting from electrophysiology measurement of α-hemolysin conductance in a suspended lipid bilayer. This

[*]Corresponding Authors Craig A. Aspinwall, Address: 1306 E University Blvd. Tucson, AZ 85721, aspinwal@email.arizona.edu, Phone: 520-621-6338; Christopher A. Baker, Address: 1420 Circle Drive, Knoxville, TN 37996, chris.baker@utk.edu, Phone: 865-974-8225.

Author Contributions

The manuscript was written through contributions of all authors. All authors have given approval to the final version of the manuscript.

ASSOCIATED CONTENT

Supporting Information. The following files are available free of charge.

Additional data related to valve characterization and performance and structures of silanes used in this work.

The authors declare no competing financial interest.

approach is well-suited for the design of novel microfluidic architectures that integrate fluidic manipulations with electrophysiological or electrochemical measurements.

Graphical Abstract

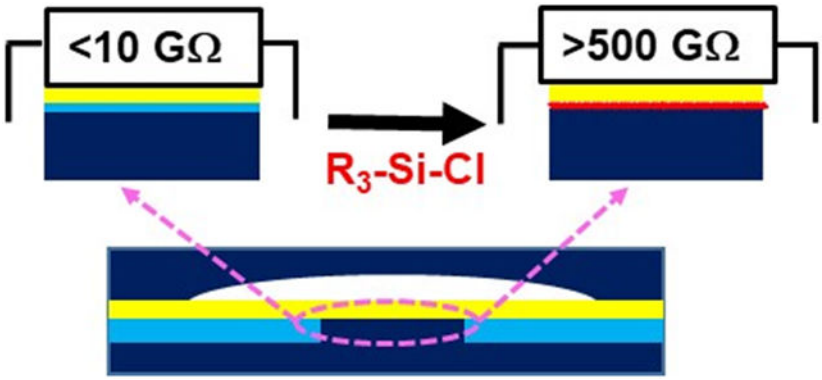

Keywords

microfluidic valve; surface modification; electrical resistance; surface energy; electrochemical properties

INTRODUCTION

Microfluidic devices offer advantages over their bench-scale counterparts, making them highly desirable in biomedical applications. Small volume systems drastically decrease sample and reagent consumption, reduce mixing and reaction times, and are amenable to a high degree of system automation which enables portable, cost-effective, and high-throughput analyses. Microfluidic systems have been widely used in biological analyses, such as polymerase chain reaction (PCR),[1-2] DNA analysis,[3-4] cell analysis,[5-6] and protein separation.[7-8] However, the continued development of miniaturized integrated analysis systems requires the development of microfluidic components with superior performance.[9]

Microfluidic valves are essential components of integrated microfluidic systems. They can be used individually or combined in series to form micro-pumps to provide various types of fluid control on chip to enable complex tasks, such as reliable sample injection,[10-11] reagent mixing,[12-13] sample sorting,[14-15] and fluid delivery.[16-17] The large variety of valve designs allows these miniaturized valves to be operated electrokinetically,[18-19] pneumatically,[20-21] and thermally,[22-23] which greatly broadens the versatility and application.

Microfluidic valves used for different applications can vary drastically in design and properties. For instance, valves actuated pneumatically for fast and precise control of operations[24] exhibit millisecond response times compared to seconds to minutes of actuation time for thermal-activated valves favored for their simplicity in design and integration.[22-23] There is no single metric that is used to compare the performance of all microfluidic valves across the board. Therefore, the outcome of the resulting application plays a key role in evaluating the microfluidic valve performance. The ability to form a high quality seal that

prevents even minute quantities of fluid from flowing, a characteristic that we term sealability, is the common function of all microfluidic valves, and thus presents an important metric for evaluating microfluidic valve performance.

Although important, sealability is often under-evaluated. Sealability can be evaluated visually by the operation of valves filled with dye solutions,[24, 25] but this approach is neither accurate nor sensitive in monitoring small degrees of leakage. On the other hand, electrical evaluation can provide sensitive, real-time characterization of microfluidic valve performance, which can be particularly useful in developing integrated microfluidic systems for electrochemical analyses. Electrical resistances of microfluidic valves in their closed states are direct measurements of valve sealability, enabling design optimization that can greatly influence device performance and experimental results.

Electrical resistance of microfluidic valves represents a limiting factor in the development of microfluidic systems for electrochemical measurements. To date, electrical resistances of microfluidic valves have predominantly been evaluated for polydimethylsiloxane (PDMS) valves, and have been reported between 2-10 GΩ.[26-28] For applications in which pA currents are measured, such as bioelectrochemistry, electrophysiology, and single-electron transport, higher seal resistance may be required.

Multiple approaches have been investigated to increase valve sealability, and thus electrical resistance. Chen et al. evaluated the effect of fluid channel size, channel aspect ratio, and PDMS diaphragm thickness on electrical resistance of a magnet-actuated PDMS push-down valve.[28] For pneumatic-actuated valves, pressure applied to close the valve has also been studied as a factor of electrical resistance.[26-27] However, surface chemistry of the valve seat, a crucial factor in achieving high quality sealing, has not, to our knowledge, been investigated as a tool to increase electrical resistance, and thus sealability, of microfluidic valves.

In this study, we explored the effect of surface chemistry of the glass valve seat on electrical resistance of pneumatically-actuated PDMS/glass microfluidic valves. Glass substrates were modified with hydrophobic silanes to decrease the surface energy of the valve seats to more closely match that of PDMS. Electrical performances of microfluidic valves with unmodified glass valve seats and hydrophobic valve seats were evaluated and compared. The utility of these surface modified microfluidic valves was demonstrated via electrophysiological measurements, in which the high electrical resistance of the valves enabled isolation of current signal resulting from ion channel reconstitution into artificial lipid bilayers.

EXPERIMENTAL

Chemicals and Materials

Chrome-coated borosilicate borofloat glass slides were purchased from Telic Co. (Santa Clarita, CA). Microposit S1813 and chrome etchant were purchased from Microchem Corp. (Westborough, MA). HF was purchased from VWR (Radnor, PA). Octyldimethylchlorosilane (ODCS) and (tridecafluoro-1,1,2,2-

tetrahydrooctyl)dimethylchlorosilane (PFDCS) were purchased from Gelest, Inc. (Morrisville, PA). Anhydrous toluene was purchased from Sigma-Aldrich (St. Louis, MO). 1,2-Diphytanoyl-*sn*-glycero-3-phosphocholine (DPhPC) was purchased from Avanti Polar Lipids, Inc. (Alabaster, AL). α-hemolysin (α-HL) was purchased from List Biological Laboratories, Inc. (Campbell, CA). H_2SO_4, H_2O_2 and KCl were purchased from EMD Chemicals, Inc. (Gibbstown, NJ). Acetone and toluene used for post-modification rinsing, and HEPES were purchased from Fisher Scientific International, Inc. (Pittsburgh, PA). HNO_3 was purchased from Macron fine chemicals (Center Valley, PA). Ethanol was purchased from Decon Laboratories, Inc. (King of Prussia, PA). PDMS sheet (0.01 inch thick, 40 durometer) was purchased from Stockwell Elastomerics, Inc. (Philadelphia, PA). N-decane was purchased from ACROS organics (Fair Lawn, NJ).

Microfluidic Valve Slide Fabrication

All photolithography was performed in the cleanroom facility in the Department of Chemistry and Biochemistry at the University of Arizona. Valve designs were printed on acrylic films by CAD/Art Services (Bandon, OR). Chrome-coated glass slides were spin coated with Microposit S1813 to obtain uniform 1.5 μm thick coatings. Valve designs were transferred to the S1813 layer using standard photolithography. The pattern was developed into the chrome layer using chrome etchant. The glass substrate was then etched in 48% HF (6 min for the channel slide, and 15 min for the displacement chamber slide). The remaining S1813 and chrome were removed by sonicating the substrates in acetone and chrome etchant for 5 min each. Finally, the valve slides were rinsed with H_2O and ethanol, and dried with compressed N_2.

Surface Modification

The surface modification procedure was adapted from solution phase modifications previously reported.[29-30] Briefly, etched valve slides were cleaned in 7:3 (v/v) H_2SO_4:H_2O_2 for 5 min, and rinsed with H_2O. Slides were then soaked in 1 M HNO_3 for 1 h, rinsed consecutively with H_2O and acetone, and dried with Ar. The activated slides were further dried at 110°C for 1 h and soaked overnight in 2% (v/v) ODCS in anhydrous toluene or PFDCS, in acetonitrile. Modified substrates were cleaned in toluene (ODCS) or acetonitrile (PFDCS), followed by acetone, H_2O and ethanol via sonication, and then dried with Ar.

Contact Angle Measurements

Contact angles were measured using a DSA 10 MK2 drop-shape analysis system (Kruss, Germany) as previously described.[30-31] A 1 μl aliquot of H_2O was dispensed manually onto the surface of interest for contact angle analysis. Contact angles were measured using sessile drop method at ten locations on each surface, and repeated for three independent surfaces per modification.

Electrical Characterization of Microfluidic Valve Operation

Microfluidic valves were assembled according to Figure 1, and filled with testing solution (1 M KCl, 5 mM HEPES at pH 7.4). Microfluidic valve operation was controlled by a 3-way micro solenoid valve (ASCO, Florham Park, NJ) toggling between vacuum (open) and

pressurized (closed) states.[20] Electrical performance was evaluated using an EPC-8 patch clamp amplifier (HEKA Electronics, Bellmore, NY) with an ITC-16 DAQ board (Instrutech, New York). Opening and closing times ($t_{10\text{-}90}$ and $t_{90\text{-}10}$, respectively) were calculated from current vs. time plots for at least 3 valves per surface modification. To measure the electrical resistance, an increasing potential was applied across the valve ranging from −100 mV to +100 mV in 10 mV increments for 100 ms per increment.[32] Resistance was calculated from the slope of *i-V* curves (n = 3). Valve opening and closing and the corresponding noise values were evaluated via application of a 10 mV holding potential.

Micropipette Fabrication

Schott glass capillaries (o.d. 1.5 mm, i.d. 1.0 mm, World Precision Instruments, Sarasota, FL) were cleaned by sonication in H_2O followed by ethanol, and dried at 60 °C for 1 h. Dried capillaries were pulled into pipets using a P-97 micropipette puller (Sutter Instrument Co., Novato, CA), and cut and fire polished using a MF-900 microforge (Narishige, East Meadow, NY) to an aperture i.d. of 15-20 μm. The pipet surface was cleaned with 1 M HNO_3 for 30 min, washed with H_2O and then dried at 110 °C for 1 h. Pipets were then silanized with PFDCS vapor for 10 min in a heated chamber.[33] Modified pipets were sequentially washed with acetonitrile, acetone, H_2O and ethanol, then dried at 60 °C for 1 h prior to use.

Lipid Membrane Formation and Ion Channel Reconstitution

DPhPC dissolved in $CHCl_3$ was dried under a stream of Ar gas then lyophilized (Labconco, Kansas City, MO) overnight. Dried lipid was resuspended in n-decane to a final concentration of 10 mg/ml. The micropipet was back filled with high K^+ solution (1 M KCl, 5 mM HEPES, pH 7.4). Black lipid membranes (BLMs) were formed across pipet tips via the tip-dip method.[34-35] Briefly, 1 μl of the DPhPC solution was applied to the solution bath 1 mm away from the tip of the pipet. The pipet was raised and lowered across the air-solution interface multiple times to facilitate BLM formation. Once the pipet resistance increased from 100 kΩ (open pipet) to > 1 GΩ, an increasing potential ranging from 0 to 1000 mV was applied to distinguish the putative BLM from multilayer lipid structures. BLM formation was confirmed by the presence of transient pores formed at higher potentials.[32] Ion channel reconstitution was accomplished by adding 0.5 μg of α-HL to bath solution (350 μl) approximately 1 mm from the pipet tip. A holding potential of −40 mV was applied across the bilayer to drive ions through the channel for electrophysiological measurements. α-HL insertions were observed as ~1 nS stepwise increases in bilayer conductance per channel.[30, 36-37]

Data Analysis

Electrophysiological data was collected and analyzed using Patchmaster v. 2.80 software (Heka Electronik). Ion channel recordings were processed in TAC X4.3.3 software (Bruxton, Seattle, WA), and filtered at 1 kHz. Numerical values are presented as mean ± standard deviation, with the exception of electrical resistances of the surface modified valves, which necessitated estimation since the resistance values obtained exceeded the measurement range of the patch clamp amplifier. All experiments were performed in triplicate on at least 3

different valve assemblies or substrates. All statistical comparisons were performed using the two-tailed Student's t-test at the 95% confidence interval.

RESULTS AND DISCUSSION

Microfluidic valves with high electrical resistance are highly desired for applications that integrate electrochemical detection or electronic communication by reducing current leakage which may lead to signal crosstalk or contribute to excessive background and/or noise in the system. Although extensive characterization of valve dimensions[28,38] and actuation mechanisms [9] have led to an overall increase in valve performance in terms of decreased fluid leakage and improved valve response times, optimization of valve electrical resistance has been less studied. Valve resistances using traditional PDMS/glass interfaces, such as those present in normally closed geometry of the Mathies valve design[38] (Figure 1) provide electrical resistances of up to 5 GΩ; however, these resistances are too low for applications that require low current (≤ pA) detection, such as ion channel measurements. Thus, improving the electrical resistance of microfluidic valves has the potential to greatly expand the development and application of integrated microfluidic devices for low current detection of biological processes.

In this work, we sought to improve the electrical resistance of PDMS/glass microfluidic valves by exploring the effect of surface chemistry. Though PDMS and glass seal sufficiently well to minimize fluid leakage and the corresponding leakage of dye molecules, the presence of a hydration layer at the glass surface leaves these flow junctions inherently permeable to ion leakage, and thus reduced electrical resistance. We hypothesized that valve seats with reduced surface energy, that more closely matched that of PDMS, would increase electrical resistance via more efficient elimination of residual aqueous solution between the valve seat and diaphragm in closed microfluidic valves.

To test this hypothesis, we modified glass valve seats with ODCS and PFDCS (structures shown in Supporting Information, Figure S2), and compared the electrical properties of surface modified and unmodified microfluidic valves. Previous study showed that ODCS and PFDCS modifications more effectively increase the water contact angle of a glass surface as compared to other silanes.[30] Microfluidic valve seat modification was confirmed by water contact angle measurements (Supporting Information, Figure S3). Unmodified glass valve seats exhibited water contact angles of 70 ± 4 ° (n = 30) after photolithography and wet etching processes. This value is higher than previously observed for piranha etched glass[30] and likely results from the complex chemical processing associated with etching. The water contact angle increased to 92 ± 3 ° (n = 30) and 99 ± 3 ° (n = 30) after ODCS and PFDCS modification, respectively, indicative of increased hydrophobicity and reduced surface energy of the valve seat substrates. PDMS diaphragms had a water contact angle of 107 ± 1 ° (n = 9), agreeing well with previous observations.[39-40] Reduced surface energy of the valve seat was anticipated to substantially improve the compatibility between PDMS and the valve seat, thus improving sealabilty and the resulting electrical resistance of the microfluidic valve.

Dynamics of Surface-modified Microfluidic Valve Operation

To evaluate their electrical properties, microfluidic valves were filled with a solution comprised of 1 M KCl, 5 mM HEPES, pH 7.4. The choice of electrolyte solution substantially influences the overall system conductivity, thus a high K^+ concentration was chosen to provide a challenge in obtaining high electrical resistance that would be commensurate with many biotechnology applications requiring electrochemical or electrophysiological detection.

We first evaluated and compared the dynamics of valve operation between unmodified, ODCS-modified, and PFDCS-modified valve seats. Current vs. time traces of valve operation are presented in Figure 2. Microfluidic valves with unmodified glass valve seats (Figure 2A) exhibited an initial sharp increase in electrical current upon actuation, followed by a slower upward drift of electrical current lasting ca. 0.5 – 1 s which ultimately led to the fully open state. This two-stage opening dynamic has been observed in other valves of similar design.[27] We suggest that the two-stage opening dynamics may result from a rapid initial deflection of the PDMS diaphragm followed by a relatively slow equilibration of ion chemistry at the glass surface as an electrical double layer is produced, although further study is needed to understand this phenomenon. Valve closure shows a similar two-stage dynamic, which we attribute to a rapid expulsion of bulk solution from the valve followed by slow thinning of the hydration layer wetting the valve seat. A momentary increase in electrical current was observed at the moment of open-to-close valve actuation, the origin of which was unclear.

Current vs time traces of valve operation for ODCS-modified and PFDCS-modified valve seats are shown in Figure 2B and 2C, respectively. A similar two-stage opening dynamic was observed for both ODCS- and PFDCS- modified valves, albeit with a more rapid second stage than observed in valves with unmodified glass valve seats. Interestingly, both silanized valves exhibited a distinct three-stage closing dynamic consisting of a rapid but modest decrease in electrical current, followed by a relatively slow downward drift in conductivity, and concluding with a rapid and substantial reduction in current to arrive in the fully closed state. The underlying mechanisms of this three-stage closing dynamic are not clear; however, the initial rapid reduction may result from the decreased volume of solution in the valve seat following application of closing pressure. The slower reduction in the second step may be due to slower exclusion of residual solution in the gap between the more hydrophobic surfaces due to lower capillary forces at the silane-modified interfaces. Finally, upon exclusion of solution from the valve seat/PDMS interface the comparable surface energy between these layers leads to rapid sealing upon direct interaction. Surprisingly, however, the thinning occurs from a state of overall higher conductivity with modified valve seats ($i > 15$ nA) as compared to unmodified glass valve seats ($i < 5$ nA). More study is needed to elucidate the mechanisms that lead to the observed open and closing dynamics in these valves; however, the observed actuation dynamics are compatible with many common valving applications.

Actuation times for bare glass and surface-modified valves were then evaluated and compared (Table 1). Opening time ($t_{10\text{-}90}$), defined as the rise time of the current trace from 10% - 90% of maximum open-valve current, was measured to be 28 ± 12 ms (n = 12) for

unmodified glass valve seats, which is consistent with previous reports of similar valve designs.[20, 41] The opening time for valves silanized with ODCS (6 ± 3 ms, n = 9) and PFDCS (5 ± 2 ms, n = 9) were statistically shorter than that of unmodified glass, which we attribute to reduced intermolecular forces between the solution and both the diaphragm and valve seat. Although, closure time (t_{90-10}) for surface-modified valves (1200 ± 490, n = 9 for ODCS-modified valves, and 980 ± 350, n = 9 for PFDCS-modified valves) were longer than that obtained for unmodified glass valves (150 ± 30 ms, n = 9) by a statistically significant amount; however, these values were still within the typical operating ranges reported for other microfluidic valves.[25, 42-43] Closure time varied greatly between individual valve assemblies for silane-modified valve seats, resulting in the large standard deviations of closure time reported in Table 1. A thorough understanding of the underlying mechanisms of valve actuation dynamics, which lies beyond the scope of the present work, will be needed to improve and optimize valve closure time. We can conclude, however, that silanized valve seats, as reported here, are better suited for applications that prioritize electrical isolation over rapid valve actuation times. Still, providing sufficient time (1-10 s) to ensure complete valve opening and closing is an accepted practice in many applications.[38] Moreover, many applications, such as electrophysiological studies, may require seconds to minutes of electrochemical recording,[36, 44] in which case closure times on the order of low seconds will not pose a significant limitation.

Electrical Characterization of Surface-modified Microfluidic Valve Assemblies

Valves with >10 GΩ, and preferably > 500 GΩ, resistance are desired to isolate small current signals (pA to nA) in many electrochemical applications. For example, with a holding potential (V_h) of 50 mV, a 10 GΩ valve resistance yields leakage currents of 5 pA, compared to 0.1 pA for a 500 GΩ valve resistance. Typical ion channel currents are in the 1 – 50 pA range.

Electrical resistances of microfluidic valves with unmodified and silanized valve seats are compared in Table 1. Valves with unmodified glass valve seats yielded electrical resistance of 7 ± 3 GΩ (n = 9), agreeing well with previous reports for pneumatic PDMS diaphragm valves.[26-27] Resistance values for unmodified glass valve seats were calculated from slopes of i-V curves (Figure 3, squares). Electrical current measured across the closed valve increased with increasing applied potential, indicating ion current leakage at the valve seat/diaphragm interface. However, current did not increase with increasing applied potential for silane-modified valve seats (Figure 3, diamonds and triangles), remaining near the noise limit for these measurements. Thus, electrical resistance was too high to be reliably calculated from the slope of these i-V curves. Based on the observed noise level of steady-state current recordings under fixed holding potentials, we estimated 500 GΩ to be the highest resistance that could be reliably measured with the patch clamp amplifier utilized in these studies. Therefore, we estimate the electrical resistance of both silane surface-modified valves to be > 500 GΩ (n = 9). Thus, silanization of glass valve seats with either ODCS or PFDCS achieved > 70-fold increase in electrical resistance, which supported the hypothesis that ODCS- and PFDCS- modified valve seats improved the elimination of a conductive hydration layer at the valve seat/diaphragm interface. The resulting microfluidic valves with

hundreds of GΩ resistance have high potential for isolating low current electrochemical signals.

Silanization of glass valve seats provided only a surface monolayer of ODCS or PFDCS. We evaluated the robustness of valve performance against repeated valve actuations to determine whether the mechanical stress of diaphragm-to-valve seat contact would impact the monolayer modification and the resulting electrical properties. Specifically, we evaluated the ability to retain the initial closed-state resistance after multiple cycles of valve actuation. Electrical resistances of silanized valves in the closed state were measured after every ten cycles of actuations, and resistance values were normalized to resistance measured on the first cycle of actuation (Supporting Information, Figure S4). No statistically significant variation in electrical resistance was observed over > 40 cycles of operation. While this study was limited to 40 actuation cycles, valves were routinely operated for >100 cycles in other experiments with no observed aberrant effects on electrical conductivity of the closed valves (data not shown).

In summary, electrical resistance increased > 70-fold for microfluidic valves with both ODCS- and PFDCS- modified valve seats. We attribute increased resistance to the effective elimination of aqueous solution at the diaphragm/valve seat interface as a result of decreased surface energy of the silanized glass substrate. A 5-fold reduction in valve opening times and statistically significant reductions in RMS noise were also observed for silanized valve seats. High electrical resistance and improved noise characteristics present opportunities for integrating surface-modified microfluidic valves with electrochemical detection of signals in pA to nA regime.

Electrical Isolation of Ion Channel Signals

To demonstrate the utility of surface-modified valve seats for isolating low current signals, we evaluated the efficacy of silanized microfluidic valves for electrically isolating electrochemical measurements. Electrophysiological monitoring of ion channel reconstitution into a synthetic lipid bilayer was chosen as a model measurement, since the low magnitude of ion current in this system provides a greater challenge for microfluidic valve resistance than many electrochemical signals. A synthetic lipid bilayer was formed at the tip of a PFDCS- modified glass micropipette, and alpha-hemolysin (α-HL) was added to the bath solution to allow spontaneous reconstitution into the bilayer. α-HL is a bacteria-derived pore forming protein commonly used in ion channel sensor platforms,[37, 45-46] and in the characterization of BLMs.[30, 36] To validate the sealability of the valve, the reference electrode and recording electrodes were placed in fluid reservoirs on opposite sides of the valve seat. Thus the path of conductance was through the valve.

The insertion of α-HL into the bilayer was monitored via current measurement under a constant bias potential of −40 mV. Each pore insertion resulted in a step of *ca.* −40 pA in the current vs. time trace (Figure 4A), which was equivalent to a conductance of *ca.* 1 nS per α-HL pore, agreeing well with previous reports of α-HL conductance.[30, 36-37] Figure 4B shows the all-points histogram of the insertions shown in Figure 4A, illustrating discrete current changes and well-resolved 1 nS conductance characteristic of α-HL insertions. α-HL

reconstitution was allowed to proceed for several minutes until the ion conductance reached a steady state.

PFDCS-modified valve seats were used to evaluate the efficacy in isolating the electrophysiology signals. The current vs. time trace for a valve operated in series with an α-HL-functionalized BLM is shown in Figure 4C. Figure 4D shows the all-points histogram for the experiment illustrated in Figure 4C. The conductance state of the α-HL functionalized BLM, measured with the valve in the open state, is well-resolved from the current baseline achieved when the microfluidic valve was in the closed state. In this case, BLM conductance was −520 ± 4 pA (n = 6), which corresponds to the insertion of 13 α-HL pores. The measured current when the valve was closed was 0.3 ± 0.1 pA (n = 6), which corresponded to the noise limit of the patch clamp amplifier operated under these conditions. Signal isolation such as this is possible only when ion current through the closed valve is significantly lower than that through the α-HL functionalized BLM, making the valve the current-limiting element of the series circuit. As such, surface-modified microfluidic valves present the opportunity to develop novel microfluidic architectures that integrate fluid manipulations with electrochemical measurements.

CONCLUSIONS

In this work, the surface energy of the valve seat component of hybrid PDMS/glass microfluidic valves was investigated as a tool to increase the electrical resistance of microfluidic valves. Upon surface modification of the glass valve seat with hydrophobic silanes, OCDS and PFDCS, that more closely match the surface energy of PDMS, and reduced valve opening time. Electrical performance was sufficiently enhanced to enable electrical isolation in electrophysiology measurements of ion conductance via α-HL pores.

Although further work is required to elucidate specific mechanisms of improved performance in these valves, the current work demonstrates a facile approach to preparing microfluidic valves capable of achieving electrical isolation of electrochemical signals in the pA regime via fluidic manipulations. This capability presents the opportunity for new functionality in integrated microfluidics, such as utilizing microfluidic valves for frequency modulation in electrochemical measurements in a manner analogous to an optical chopper. Additionally, we foresee the potential for these valves to enable highly multiplexed electrochemical measurements from a single potentiostat or amplifier. In general, the ability to achieve high quality electrical isolation via fluidic manipulation presents a new tool in the design and development of integrated microfluidic systems for electrochemical measurements.

Supplementary Material

Refer to Web version on PubMed Central for supplementary material.

ACKNOWLEDGMENTS

This research was supported by National Institutes of Health via the National Institute of Biomedical Imaging and Bioengineering under Grant No. 2R01EB007047 and 1R21EB022297 and the National Institute of General Medical

Sciences under Grant No. 1R01GM095763. The content is solely the responsibility of the authors and does not necessarily represent the official views of the sponsors.

REFERENCES

(1). White AK; Vanlnsberghe M; Petriv OI; Hamidi M; Sikorski D; Marra MA; Piret J; Aparicio S; Hansen CL High-Throughput Microfluidic Single-Cell RT-qPCR. Proc. Natl. Acad. Sci. U. S. A 2011, 108, 13999–14004. [PubMed: 21808033]

(2). Liu J; Enzelberger M; Quake S A Nanoliter Rotary Device for Polymerase Chain Reaction. Electrophoresis. 2002, 23, 1531–1536. [PubMed: 12116165]

(3). Zhang Y; Park S; Yang S; Wang TH An All-in-one Microfluidic Device for Parallel DNA Extraction and Gene Analysis. Biomed. Microdevices 2010, 12, 1043–1049. [PubMed: 20632111]

(4). Paegel BM; Blazej RG; Mathies RA Microfluidic Devices for DNA Sequencing: Sample Preparation and Electrophoretic Analysis. Curr. Opin. Biotechnol 2003, 14, 42–50. [PubMed: 12566001]

(5). Wheeler AR; Throndset WR; Whelan RJ; Leach AM; Zare RN; Liao YH; Farrell K; Manger ID; Daridon A Microfluidic Device for Single-Cell Analysis. Anal. Chem 2003, 75, 3581–3586. [PubMed: 14570213]

(6). Grabowski M; Buchenauer A; Hasni AE; Klockenbring T; Barth S; Mokwa W; Schnakenberg U Microfluidic System for Cell Fusion. Procedia Eng. 2010, 5, 1332–1335.

(7). Shameli SM; Ren CL Microfluidic Two-Dimensional Separation of Proteins Combining Temperature Gradient Focusing and Sodium Dodecyl Sulfate-Polyacrylamide Gel Electrophoresis. Anal. Chem 2015, 87, 3593–3597. [PubMed: 25787346]

(8). Sarkar A; Hou HW; Mahan AE; Han J; Alter G Multiplexed Affinity-Based Separation of Proteins and Cells Using Inertial Microfluidics. Sci. Rep 2016, 6, 23589. [PubMed: 27026280]

(9). Oh KW; Ahn CH A Review of Microvalves. J. Micromech. Microeng 2006, 16, R13–R39.

(10). Jacobson SC; Ermakov SV; Ramsey JM Minimizing the Number of Voltage Sources and Fluid Reserviors for Electrokinetic Valving in Microfluidic Devices. Anal. Chem 1999, 71, 3273–3276. [PubMed: 21662916]

(11). Leach AM; Wheeler AR; Zare RN Flow Injection Analysis in a Microfluidic Format. Anal. Chem 2003, 75, 967–972. [PubMed: 12622393]

(12). Guo ZX; Zeng Q; Zhang M; Hong LY; Zhao YF; Liu W; Guo SS; Zhao XZ Valve-Based Microfluidic Droplet Micromixer and Mercury (II) Ion Detection. Sens. Actuators, A 2011, 172, 546–551.

(13). Li N; Hsu CH; Folch A Parallel Mixing of Photolithographically Defined Nanoliter Volumes Using Elastomeric Microvalve Arrays. Electrophoresis. 2005, 26, 3758–3764. [PubMed: 16196107]

(14). Sundararajan N; Kim D; Berlin AA Microfluidic Operations Using Deformable Polymer Membranes Fabricated by Single Layer Soft Lithography. Lab Chip. 2005, 5, 350–354. [PubMed: 15726212]

(15). Fu AY; Chou HP; Spence C; Arnold FH; Quake SR An Integrated Microfabricated Cell Sorter. Anal. Chem 2002, 74, 2451–2457. [PubMed: 12069222]

(16). Unger MA; Chou H; Thorsen T; Scherer A; Quake SR Monolithis Microfabricated Valves and Pumps by Multilayer Soft Lithography. Science. 2000, 288, 113–116. [PubMed: 10753110]

(17). Kim J; Kang M; Jensen EC; Mathies RA Lifting Gate PDMS Microvalves and Pumps for Microfluidic Control. Anal. Chem 2012, 84, 2067–2071. [PubMed: 22257104]

(18). Schasfoort RBM; Schlautmann S; Hendrikse J; van den Berg A Field-Effect Flow Control for Microfabricated Fluidic Networks. Science. 1999, 286, 942–945. [PubMed: 10542145]

(19). Kirby BJ; Shepodd TJ; Hasselbrink EF Jr. Voltage-Addressable On/OFF Microvalves for High-Pressure Microchip Separations. J. Chromatogr. A 2002, 979, 147–154. [PubMed: 12498243]

(20). Zhang W; Lin S; Wang C; Hu J; Li C; Zhuang Z; Zhou Y; Mathies RA; Yang CJ PMMA/PDMS Valves and Pumps for Disposable Microfluidics. Lab Chip. 2009, 9, 3088–3094. [PubMed: 19823724]

(21). Gu P; Liu K; Chen H; Nishida T; Fan ZH Chemical-Assisted Bonding of Thermoplastics/ Elastomer for Fabricating Microfluidic Valves. Anal. Chem. 2011, 83, 446–452. [PubMed: 21121689]

(22). Wang J; Chen Z; Mauk M; Hong KS; Li M; Yang S; Bau HH Self-Actuated, Thermo-Responsive Hydrogel Valves for Lab on a Chip. Biomed. Microdevices 2005, 7, 313–322. [PubMed: 16404509]

(23). Yang B; Lin Q A Latchable Microvalve Using Phase Change of Paraffin Wax. Sens. Actuators, A 2007, 134, 194–200.

(24). Lau ATH; Yip HM; Ng KCC; Cui X; Lam RHW Dynamics of Microvalve Operations in Integrated Microfluidics. Micromachines. 2014, 5, 50–65.

(25). Gu W; Chen H; Tung Y-C; Meiners J-C; Takayama S Multiplexed Hydraulic Valve Actuation Using Ionic Liquid Filled Soft Channels and Braille Displays. Appl. Phys. Lett 2007, 90, 033505.

(26). Kartalov EP; Maltezos G; Anderson WF; Taylor CR; Scherer A Electrical Microfluidic Pressure Gauge for Elastomer Microelectrochemical Systems. J. Appl. Phys 2007, 102, 84909–849094. [PubMed: 19587835]

(27). Chen H; Gu W; Cellar N; Kennedy R; Takayama S; Meiners J-C Electromechanical Properties of Pressure-Actuated PDMS Microfluidic Push-Down Valves. Anal. Chem 2008, 80, 6110–6113. [PubMed: 18576665]

(28). Chen C-Y; Chen C-H; Tu T-Y; Lin C-M; Wo AM Electrical Isolation and Characteristics of Permanent Magnet-Actuated Valves for PDMS Microfluidics. Lab Chip. 2011, 11, 733–737. [PubMed: 21132206]

(29). Cras JJ; Rowe-Taitt CA; Nivens DA; Ligler FS Comparison of Chemical Cleaning Methods of Glass in Preparation for Silanization. Biosens. Bioelectron 1999, 14, 683–688.

(30). Bright LK; Baker CA; Agasid MT; Ma L; Aspinwall CA Decreased Aperture Surface Energy Enhances Electrical, Mechanical, and Temporal Stability of Suspended Lipid Membranes. ACS Appl. Mater. Interfaces 2013, 5, 11918–11926. [PubMed: 24187929]

(31). Ross EE; Rozanski IJ; Spratt T; Liu SC; O'Brien DF; Saavedra SS Planar Supported Lipid Bilayer Polymers Formed by Vesicle Fusion. 1. Influence of Diene Monomer Structure and Polymerization Method on Fil, Properties. Langmuir. 2003, 19, 1752–1765.

(32). Heitz BA; Xu J; Jones IW; Keogh JP; Comi TJ; Hall HK; Aspinwall CA; Saavedra SS Polymerized Planar Suspended Lipid Bilayers for Single Ion Channel Recordings: Comparison of Several Dienoyl Lipids. Langmuir. 2011, 27, 1882–1890. [PubMed: 21226498]

(33). Bright LK; Baker CA; Bränström R; Saavedra SS; Aspinwall CA Methacrylate Polymer Scaffolding Enhances the Stability of Suspended Lipid Bilayers for Ion Channel Recordings and Biosensor Development. ACS Biomater. Sci. Eng 2015, 1, 955–963. [PubMed: 26925461]

(34). Hanke W; Methfessel C; Wilmsen U; Boheim G Ion Channel Reconstitution into Lipid Bilayer Membranes on Glass Patch Pipettes. Bioelectrochem. Bioenerg 1984, 12, 329–339.

(35). Agasid MT; Comi TJ; Saavedra SS; Aspinwall CA Enhanced Temporal Resolution with Ion Channel-Functionalized Sensors Using a Conductance-Based Measurement Protocol. Anal. Chem 2017, 89, 1315–1322. [PubMed: 27981836]

(36). White RJ; Ervin EN; Yang T; Chen X; Daniel S; Cremer PS; White HS Single Ion-Channel Recordings Using Glass Nanopore Membranes. J. Am. Chem. Soc 2007, 129, 11766–11775. [PubMed: 17784758]

(37). Deamer DW Characterization of Nucleic Acids by Nanopore Analysis. Acc. Chem. Res 2002, 35, 817–825. [PubMed: 12379134]

(38). Grover WH; Skelley AM; Liu CN; Lagally ET; Mathies RA Monolithic Membrane Valves and Diaphragm Pumps for Practical Large-Scale Integration into Glass Microfluidic Devices. Sens. Actuators, B 2003, 89, 315–323.

(39). He Z; Ma M; Lan X; Chen F; Wang K; Deng H; Zhang Q; Fu Q Fabrication of Transparent Superamphiphobic Coating with Improved Stability. Soft Matter. 2011, 7, 6435–6443.

(40). Chuah YJ; Koh YT; Lim K; Menon NV; Wu Y; Kang Y Simple Surface Engineering of Polydimethylsiloxane with Polydopamine for Stabilized Mesenchymal Stem Cell Adhesion and Multipotency. Sci. Rep 2015, 5, 18162. [PubMed: 26647719]

(41). Rogers CI; Oxborrow JB; Anderson RR; Tsai L; Nordin GP; Woolley AT Microfluidic Valves Made from Polymerized Polyethylene Glycol Diacrylate. Sens. Actuators, B 2014, 191, 438–444.

(42). Kim JH; Na KH; Kang CJ; Jeon D; Kim YS A Disposable Thermopneumatic-Actuated Microvalve Stacked with PDMS Layers and ITO-Coated Glass. Microelectron. Eng 2004, 73-74, 864–869.

(43). Baek JY; Park JY; Ju JI; Lee TS; Lee SH A Pneumatically Controllable Flexible and Polymeric Microfluidic Valve Fabricated via In Situ Development. J. Micromech. Microeng. 2005, 15, 1015–1020.

(44). Zakharian E Recording of Ion Channel Activity in Planar Lipid Bilayer Experiments. Methods Mol Biol. 2013, 998, 109–118. [PubMed: 23529424]

(45). Clarke J; Wu H; Jayasinghe L; Patel A; Reid S; Bayley H Continuous Base Identification for Single-Molecule Nanopore DNA Sequencing. Nat. Nanotechnol 2009, 4, 265–270. [PubMed: 19350039]

(46). Reiner JE; Balijepalli A; Robertson JWF; Campbell J; Suehle J; Kasianowicz JJ Disease Detection and Management via Single Nanopore-Based Sensors. Chem. Rev 2012, 112, 6431–6451. [PubMed: 23157510]

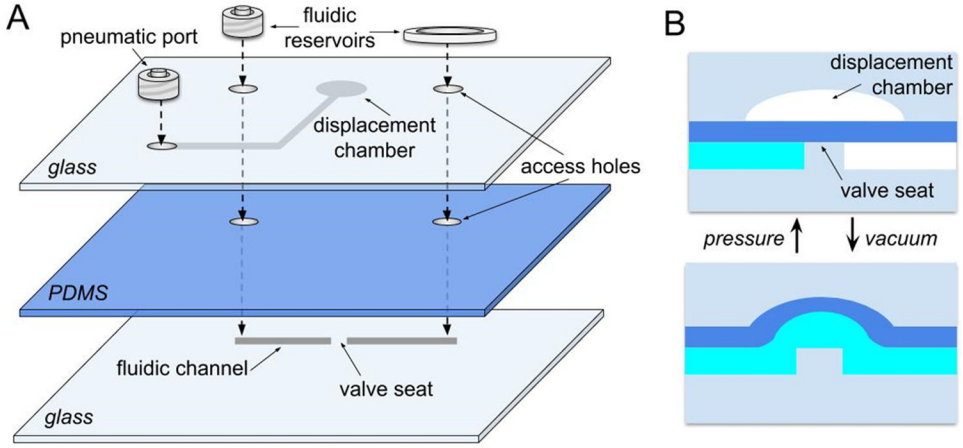

Figure 1. Schematic of PDMS/Glass Pneumatic Valve Design.

A. Exploded view of microfluidic device assembly. A 250 μm thick PDMS diaphragm layer is sandwiched between a glass pneumatic layer (top) and a glass fluidic layer (bottom) which includes the valve seat. The valve seat dimensions: 620 μm (l) x 130 μm (w). **B.** Cross-sectional view of valve operation. The valve is maintained in the closed state via pressure application of 60 kPa (see Supporting Information, Figure S1) applied to the displacement chamber.[20] Vacuum application at the displacement chamber results in the open valve state by displacing the PDMS diaphragm.

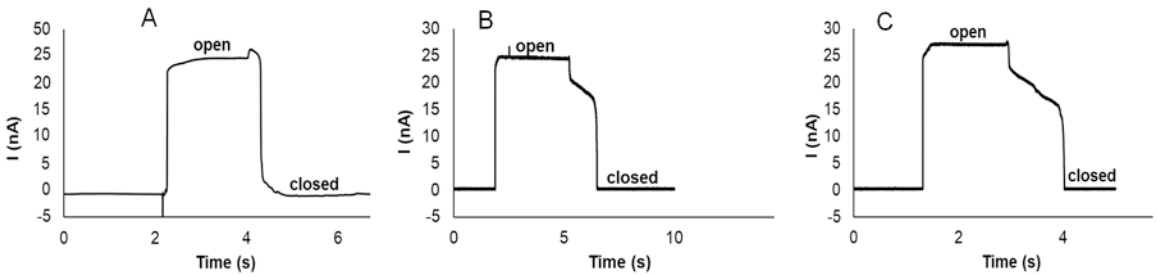

Figure 2. Current vs. time traces of microfluidic valve operation

A. Unmodified glass valve seat **B.** ODCS-modified valve seat **C.** PFDCS-modified valve seat. In all cases, rapid increases in current signal were observed when the valves were switched from closed state to open state. When switched from open state to closed state, PFDCS- and ODCS- modified valves exhibited 3-step closings which were not observed in unmodified valves. V_h = 10 mV.

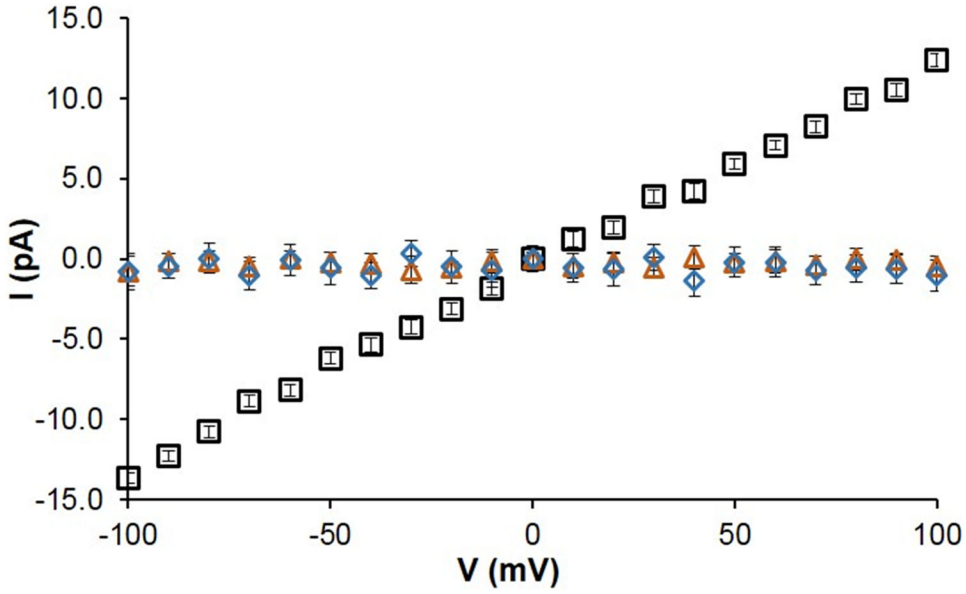

Figure 3. I-V curves for microfluidic valves in the closed state.

Increasing electrical current was observed with increasing voltage application for unmodified glass valve seats (squares), indicating ion current leakage across the closed valve. ODCS-modified valves (diamonds) and PFDCS-modified valves (triangles) showed no evidence of ion current.

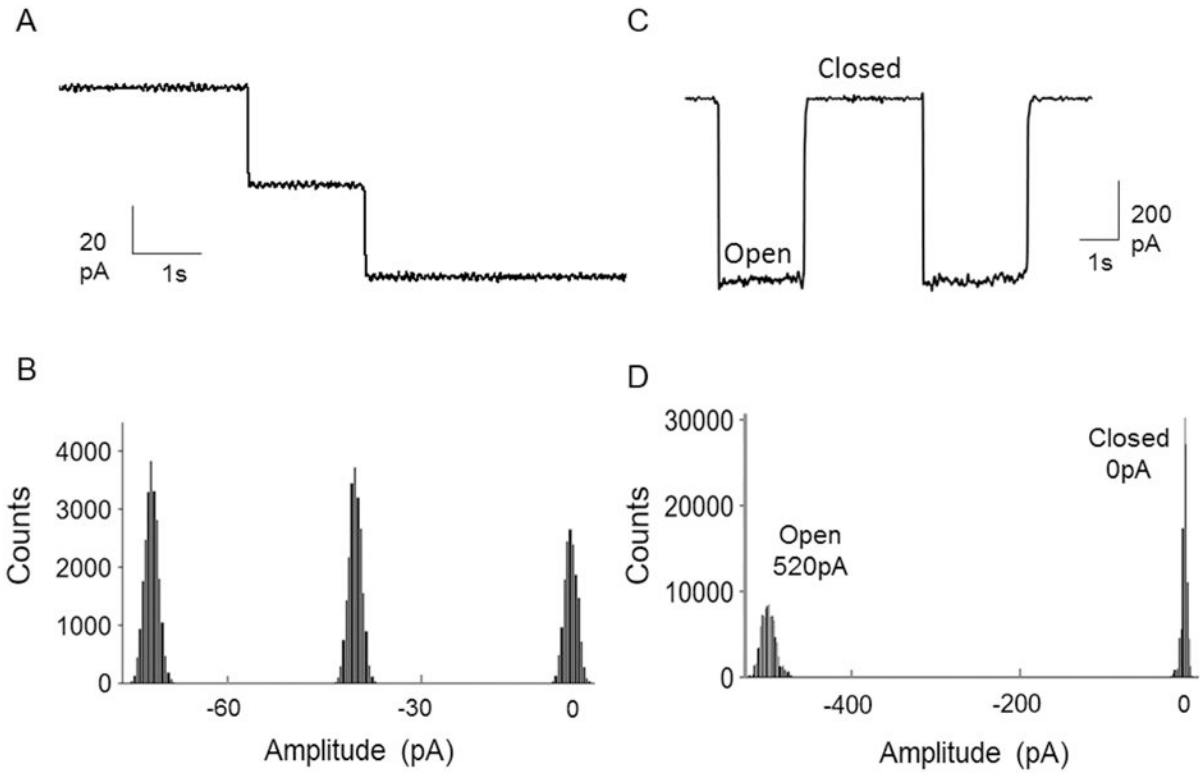

Figure 4. Electrical isolation of low amplitude electrophysiological signals

A. Step changes of ca. −40 pA in the current vs. time trace indicate the insertion of individual α-HL pores into a synthetic lipid bilayer **B.** The all-points histogram of the data in panel A is shown. Single ion channel resolution is evident via well-resolved conductance states at ca −40 pA and −80 pA. **C.** The current vs. time trace of valve operation placed in series with α-HL functionalized BLM is shown. **D.** The all-point histogram of the data in panel C is shown. The population at −520 ± 4 pA indicates a BLM functionalized with 13 α-HL pores. When the valve was closed, the detectable current is 0.3 ± 0.1 pA. BLMs for this comparison were formed on PFDCS-modified pipettes.

Table 1.

Characterization of unsilanized and silanized valves

Surface Condition	Valve Resistance (GΩ)	Opening time[a] (ms)	Closure Time[b] (ms)
Unmodified	7 ± 3	30 ± 20	150 ± 30
ODCS	> 500	6 ± 3	1200 ± 490
PFDCS	> 500	5 ± 2	980 ± 350

[a] The opening time is defined as $t_{10\text{-}90}$, the time for microfluidic valve to increase from 10% to 90% of the maximum signal.

[b] The closure time is defined as $t_{90\text{-}10}$, the time for microfluidic valve to decrease from 90% to 10% of the maximum signal